Corrections to the universal behavior of the Coulomb-blockade peak splitting for quantum dots separated by a finite barrier

John M. Golden and Bertrand I. Halperin
Department of Physics, Harvard University, Cambridge, Massachusetts 02138
(Received 21 November 1996; revised manuscript received 21 April 1997)

Building upon earlier work on the relation between the dimensionless interdot channel conductance g and the fractional Coulomb-blockade peak splitting f for two electrostatically equivalent dots, we calculate the leading small-g correction that results from an interdot tunneling barrier that is not a δ function but, rather, has a finite height V_0 and a nonzero width ξ and can be approximated as parabolic near its peak. The finiteness of the barrier leads to a small upward shift of the f-versus-g curve for $g \ll 1$. The shift is a consequence of the fact that the tunneling matrix elements vary exponentially with the energies of the states connected. For a parabolic barrier, the energy scale for the variation is $\hbar\omega$, where ω, which is proportional to $\sqrt{V_0}/\xi$, is the harmonic oscillator frequency of the inverted parabolic well. In the limit $g \to 0$, the finite-width f-versus-g curve behaves like $(U/\hbar\omega)/|\ln g|$, where U is the energy cost associated with moving electrons between the dots. [S0163-1829(97)06032-3]

I. INTRODUCTION

The opening of tunneling channels between two quantum dots leads to a transition from a Coulomb blockade characteristic of isolated dots to one characteristic of a single large composite dot.[1] For electrostatically identical dots characterized by charging energies U much greater than their single-particle level spacings δ_{2D}, this transformation can be chronicled by tracking the splitting of the Coulomb-blockade conductance peaks as a function of the conductance through the interdot tunneling channels.[2–4] If one assumes a single common value for the conductance in each tunneling channel (an assumption exactly fulfilled for a spin-symmetric system of only two channels, one for spin-up electrons and the other for spin-down electrons), one can divide the peak splitting by its saturation value and look for the relation between two dimensionless quantities:[5,6] the fractional peak splitting f and the dimensionless channel conductance g.[7]

For $g \ll 1$, prior work[5,6,8,9] has treated the coupled-dot problem via a ''transfer-Hamiltonian approach,''[10] in which hopping elements connect states localized on one dot to those localized on the other. (Here *localized* signifies that a state is entirely restricted to one of the dots.) The hopping elements have been treated as constant, independent of the states connected, as they would be if the interdot barrier were a δ function. For such a barrier, the leading small-g behavior of f is given by $f^{(1)}_{\xi=0} = (2\ln 2/\pi^2) N_{\rm ch} g$, where $N_{\rm ch}$ is the number of separate tunneling modes (spin-up and spin-down channels are counted separately). The superscript of $f^{(1)}_{\xi=0}$ tells us that this is the leading term in the weak-coupling limit. The subscript further specifies that this term is calculated for a tunneling barrier of effectively zero width ($\xi = 0$) and therefore, by implication, of infinite height. For $g \gtrsim 0.2$, terms that are higher order in g contribute significantly to the zero-width splitting; the terms proportional to g^2 have been calculated in previous work.[6]

In this paper, we calculate a different correction to $f^{(1)}_{\xi=0}$ which arises from the fact that a realistic barrier possesses a finite height V_0 and a nonzero width ξ. For such a barrier, the hopping elements are not independent of the states they connect, and, for small g, they depend exponentially on the energies of the states. Hence, in the weak-coupling limit ($g \ll 1$), it can pay to tunnel to intermediate states with energies above the barrier. The leading term in f then behaves as $(U/W)/|\ln g|$, where U measures the capacitive energy cost of moving electrons between the dots and W is the characteristic energy scale over which the hopping elements change from their values at the Fermi energy.

We examine specifically the case of a finite-width barrier that can be treated as parabolic near its peak. For such a barrier, the energy scale W is equal to $\hbar\omega/2\pi$, where ω is the harmonic oscillator frequency of the inverted parabolic well. This frequency is proportional to the square root of the barrier curvature, itself proportional to V_0/ξ^2. It follows that the limit $\xi \to 0$ corresponds to the limit $U/W \to 0$. In recent experiments,[2–4] however, it appears that U/W is roughly 1. Under such circumstances, the fractional peak splitting f is larger than the zero-width splitting, $f_{\xi=0}$, by a small but noticeable amount, and, in the extreme limit of $g \to 0$, the ratio of the finite-width splitting to the previously calculated zero-width splitting is very large. For intermediate values of g, the effect of $\xi \neq 0$ is less dramatic, the primary effects being a relatively small increase in f and a reduction in the slope of the f-versus-g curve.

To find the leading term in the finite-width peak splitting we adopt a *stationary-state approach*,[10] in which the first step is to solve for the single-particle eigenstates of noninteracting electrons that move in the electrostatic potential of the coupled dots. The capacitive interactions between the electrons are expressed in terms of these noninteracting double-dot eigenstates, and the off-diagonal elements are treated perturbatively. The leading term in the finite-width fractional peak splitting, $f^{(1)}$, is determined by finding the value for $\rho = 1$ of a more general quantity $\tilde{f}^{(1)}(\rho)$, where ρ is a dimensionless parameter which measures the bias asymmetry between the dots.[5,6] In the limit $U/W \to 0$, the

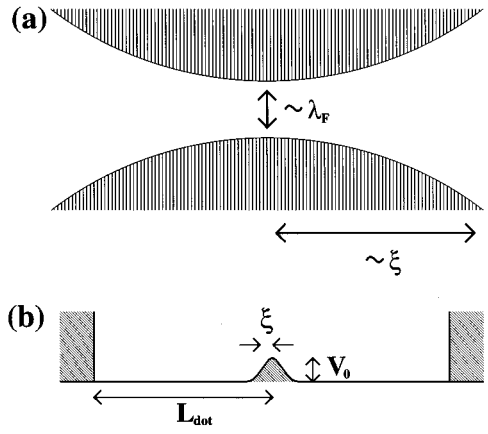

FIG. 1. (a) Schematic diagram for a single orbital-mode connection between the two dots. Over a distance of order ξ, the connection narrows to a minimum width on the order of the Fermi wavelength λ_F. (b) ''Boxlike'' double-dot system with a central barrier. Hard confining walls are at a distance $L_{\rm dot}$ from the barrier, which is of height V_0 and half width ξ.

zero-width result, $f^{(1)}_{\xi=0}$, is recovered. For finite U/W, an approximate analytic calculation demonstrates the limiting $1/|\ln g|$ behavior. For the particular choice $U/W=1$, as well as for various other choices of the ratio U/W, the leading term in the fractional peak splitting is computed numerically as a function of g. For $U/W\simeq 1$, previous predictions for the splitting at intermediate g are essentially unaltered.

The structure of this paper is as follows. Section II develops the stationary-state approach for calculating $\tilde{f}(\rho)$. Section III implements this approach for a parabolic interdot barrier, verifying the $(U/W)/|\ln g|$ behavior of the $g\to 0$ peak splitting for $\xi\neq 0$ and putting the finite-width calculation in the context of earlier work. Section IV summarizes the results and speculates on the effect of $\xi\neq 0$ when the dots are strongly coupled ($g\simeq 1$).

II. THE STATIONARY-STATE APPROACH

We make the problem one-dimensional (1D) by considering a smooth, adiabatic interdot connection [see Fig. 1(a)] which, for simplicity, we presume to contain only one transverse orbital mode that lies near or below the Fermi energy.[11] (The use of one orbital mode corresponds to the spin-symmetric $N_{\rm ch}=2$ experiments of Waugh *et al.*,[2] Crouch *et al.*,[3] and Livermore *et al.*[4]) For such a connection, the only parts of an electron wave function that can pass from dot to dot are those that overlap with the lowest transverse mode. Hence, in investigating the effect of the connection, we can ignore all electrons but those in this lowest mode. We are left with a 1D problem in which a representative electron moves in an effective potential $V(x)=E_{\rm tr}(x)+V_{\rm el}(x)$, where $E_{\rm tr}(x)$ is the spatially dependent kinetic energy of the lowest transverse mode and $V_{\rm el}(x)$ is the spatially dependent electrostatic energy. The characteristic length scale for the spatial variation of $V(x)$ is the ''barrier width'' ξ.

For computational convenience, we employ hard boundaries at a distance $L_{\rm dot}$ from the barrier, giving us a ''boxlike'' double dot with a smoothly varying longitudinal potential [see Fig. 1(b)]. The details of the boundary conditions away from the connecting region are unimportant so long as the connecting region itself is sufficiently smooth.[12]

The Hamiltonian consists of two components. The first, H_0, is a diagonal term that gives the energies of the noninteracting, single-particle eigenstates. The second, $H_C=U(\hat{n}-\rho/2)^2$, gives the capacitive energy cost of moving electrons from one side of the barrier to the other.[5,6] Here, $\hat{n}$ counts the electrons transferred from dot 1 to dot 2 (assuming, for convenience, an even total number of electrons initially divided equally between the two dots). The parameter ρ measures the capacitively weighted interdot bias.[5,6]

For the noninteracting electrons characterized by H_0, the dimensionless channel conductance g is the transmission probability for a particle incident on the barrier at the Fermi energy.[10] f is not so easily determined because, in its evaluation, H_C is relevant. Thus, we must develop a means of dealing with $\hat{n}$, which is not diagonal in the basis of noninteracting single-particle eigenstates.

Our strategy is to switch to a basis that renders $\hat{n}$ nearly diagonal at energies that are low compared to the barrier. We use the fact that, for a bound system containing two equal potential minima, the eigenstates come in well-defined, discrete pairs of opposite parity. Hence, we write $H_0=\Sigma_{\sigma,j}E_S(j)c^\dagger_{Sj\sigma}c_{Sj\sigma}+\Sigma_{\sigma,j}E_A(j)c^\dagger_{Aj\sigma}c_{Aj\sigma}$, where S and A are the even and odd parity indices, j is the pair index, and σ is the spin index (or, more generally, a channel index).

At lower and lower energies relative to the barrier, the splitting within the pairs, $|E_A(j)-E_S(j)|$, approaches zero, but the spacing between pairs, $|E_S(j+1)-E_A(j)|$, remains approximately equal to δ_{1D}, where $\delta_{1D}=\pi\hbar v_F/L_{\rm dot}$ (assuming we do not stray too far from the Fermi surface), v_F being the Fermi velocity. At low energies, one can form doublets of *quasilocalized* states—states that lie mostly on one of the two sides of the central barrier—from linear combinations of the members of each eigenstate pair. If $\phi_{Sj}(x)$ and $\phi_{Aj}(x)$ are the real symmetric and antisymmetric eigenfunctions of the jth lowest-energy pair (with appropriately chosen overall phases), the recipe is $\Omega_{j\alpha}(x)=(1/\sqrt{2})[\phi_{Sj}(x)+(-1)^{\alpha+1}\phi_{Aj}(x)]$, where the dot index α signifies that $\Omega_{j\alpha}(x)$ is primarily localized on the dot 1 side of the barrier if $\alpha=1$ and on the dot 2 side if $\alpha=2$.

At high energies, we continue to form the analogous combinations. We refer to the full set of states $\Omega_{j\alpha}(x)$ as *semilocalized* to indicate that these states are sometimes quasilocalized (i.e., at low energies) and sometimes not.

The semilocalized states are the basis needed. In terms of the associated annihilation operators $a_{j\alpha\sigma}=(1/\sqrt{2})[c_{Sj\sigma}+(-1)^{\alpha+1}c_{Aj\sigma}]$, we have $H_0=\Sigma_{\sigma,\alpha,j}E(j)a^\dagger_{j\alpha\sigma}a_{j\alpha\sigma}-\Sigma_{\sigma,j}t(j)(a^\dagger_{j2\sigma}a_{j1\sigma}+\text{H.c.})$, where $E(j)$ is the average energy of the pair and $t(j)$ is half the difference within the pair. Whereas $E(j)$ is generally on the order of the Fermi energy, $t(j)$ is no greater than the average level spacing $\delta_{1D}=\pi\hbar v_F/L_{\rm dot}$ and vanishes in the large-dot limit ($L_{\rm dot}\to\infty$). The minuteness of $t(j)$ permits us to ignore it in calculating the leading contribution to f.

We write $\hat{n}$ in terms of the semilocalized operators. If dot

1 corresponds to the $x<0$ side of the barrier and dot 2 corresponds to the $x>0$ side, we have $\hat{n}=(1/2)\int dx[\Theta(x)-\Theta(-x)]\psi^{\dagger}(x)\psi(x)$, where $\psi(x)$ is the position operator and $\Theta(x)$ is the Heaviside step function. After writing $\psi(x)$ in terms of the $a_{j\alpha\sigma}$, we see that $\hat{n}=\hat{n}_0+\delta\hat{n}_C+\delta\hat{n}_T$, where $\hat{n}_0=\Sigma_{\sigma,\alpha,j}[(-1)^{\alpha}/2]a^{\dagger}_{j\alpha\sigma}a_{j\alpha\sigma}$, $\delta\hat{n}_C$ does not transfer electrons from dot 1 to dot 2, and $\delta\hat{n}_T$ does effect such a transfer:

$$\delta\hat{n}_C=\sum_{\sigma,\alpha,j_1,j_2}\left[B(j_2,\alpha;j_1,\alpha)-\frac{(-1)^{\alpha}}{2}\delta_{j_1,j_2}\right]a^{\dagger}_{j_2\alpha\sigma}a_{j_1\alpha\sigma},$$

$$\delta\hat{n}_T=\sum_{\sigma,\alpha,j_1,j_2}B(j_2,\overline{\alpha};j_1,\alpha)a^{\dagger}_{j_2\overline{\alpha}\sigma}a_{j_1\alpha\sigma}. \tag{1}$$

Here,

$$B(j_2,\alpha_2;j_1,\alpha_1)=(1/2)\int_0^{L_{\rm dot}}dx[(-1)^{\alpha_1+1}\phi_{Sj_2}(x)\phi_{Aj_1}(x)+(1\leftrightarrow 2)],$$

where $(1\leftrightarrow 2)$ indicates that the previous term is repeated with indices 1 and 2 exchanged, and $\overline{\alpha}$ means ''not α.''

Using $\delta\hat{n}=\delta\hat{n}_C+\delta\hat{n}_T$ and assuming that g is small, we express the Hamiltonian in terms of one nonperturbative piece, H_0', and two perturbative pieces, H_T' and H_C':

$$H_0'=\sum_{\sigma,\alpha,j}E(j)a^{\dagger}_{j\alpha\sigma}a_{j\alpha\sigma}+U(\hat{n}_0-\rho/2)^2,$$

$$H_T'=-\sum_{\sigma,j}t(j)(a^{\dagger}_{j2\sigma}a_{j1\sigma}+\text{H.c.}),$$

$$H_C'=U(\hat{n}_0-\rho/2)\,\delta\hat{n}+U\,\delta\hat{n}(\hat{n}_0-\rho/2)+U(\delta\hat{n})^2. \tag{2}$$

As in Refs. 5 and 6, the fractional peak splitting is determined from $\tilde{f}(\rho)$, where $\tilde{f}(\rho)=4[\Delta(0)-\Delta(\rho)]/U$, and $\Delta(\rho)$ is the energy shift of the ground state of H_0' due to the perturbations H_T' and H_C' for the given value of ρ, where $0\leqslant\rho<1$ and the total number of particles in the double dot is even. The quantity $\lim_{\rho\to 1}\tilde{f}(\rho)$ equals the fractional peak splitting f.

Since we are only interested in relative energy shifts, we can ignore terms such as $\langle 0|U(\delta\hat{n})^2|0\rangle$ that are independent of ρ. (Here the brackets indicate an expectation value taken in the ground state of H_0'.) Terms of the form $\langle 0|U(\hat{n}_0-\rho/2)\,\delta\hat{n}|0\rangle$ are zero due to the symmetry of the ground state with respect to interchange of the dots. Finally, terms that contain H_T' are negligible because $t(j)$ goes to zero with the reciprocal of the system size and, unlike $\delta\hat{n}$, H_T' only connects each state to one other, rather than connecting each state to a manifold of others. The leading perturbative energy shift is therefore

$$\Delta^{(2)}(\rho)=-U^2\left\langle 0\left|\delta\hat{n}P_0\frac{(\hat{n}_0-\rho)^2}{H_0'-E_0'(\rho)}P_0\delta\hat{n}\right|0\right\rangle, \tag{3}$$

where $E_0'(\rho)$ is the energy of the ground state of H_0' and where P_0 is the operator that projects out the unperturbed ground state. $\Delta^{(2)}(\rho)$ consists of two parts: a term second-order in $\delta\hat{n}_C$, which involves hopping between states semilocalized on the same dot, and a term second order in $\delta\hat{n}_T$, which involves hopping between states on different dots.

III. PEAK SPLITTING AND CONDUCTANCE FOR A PARABOLIC BARRIER

In order to progress further, we must adopt a model for the barrier that gives the energy dependence of the elements of $\delta\hat{n}$ [recall Eq. (1)]. We assume that the interdot barrier can be modeled as parabolic. For an energy barrier with peak height V_0, such a model is plausible when $V_0\simeq E_F\gg U$, where E_F is the Fermi energy.[13] The formula for a parabolic potential centered at the origin with half width ξ is $V(x)=V_0(1-x^2/2\xi^2)$ for $|x|<\sqrt{2}\xi$ and 0 otherwise. A crucial energy scale is the harmonic oscillator energy $\hbar\omega$ of the inverted parabolic well: $\hbar\omega=(2\pi\hbar)^2/2\pi\sqrt{2}m\lambda_V\xi$, where $2\pi/\lambda_V=(2mV_0/\hbar^2)^{1/2}$ and m is the effective mass of the electron.

The problem of transmission through a parabolic barrier is exactly solvable using parabolic cylinder functions.[14–16] The dimensionless channel conductance is[15,17] $g=1/[1+e^{-2\pi y(E_F)}]$, where E_F is the Fermi energy and $y(E)=(E-V_0)/\hbar\omega$. It follows that $(V_0-E_F)/\hbar\omega=(1/2\pi)\ln[(1-g)/g]$. Consequently, even for experimental systems[2,3] in which ξ is quite small ($\xi\simeq\lambda_F$), E_F is close to V_0 for $|\ln g|\ll 2\pi^2\sqrt{2}$.

We now consider the sizes of the energies U and W. From the result for g, the energy scale W equals $\hbar\omega/2\pi$ and $U/W=2\pi U/\hbar\omega$. For symmetric dots, U equals $e^2/(C_\Sigma+2C_{\rm int})$, where C_Σ is the total capacitance of one of the dots and $C_{\rm int}$ is the interdot capacitance.[3,5] The energy scale $\hbar\omega$ is, by comparison, only roughly known. From the fact that the barrier height V_0 is approximately equal to E_F, we know that $\lambda_V\simeq\lambda_F$. Calculations such as that of Davies and Nixon of the potential induced by a line gate[18] suggest that $\xi\simeq d$, where d is the distance between the surface metallic gates and the two-dimensional electron gas (2DEG). In the $Al_xGa_{1-x}As/GaAs$ heterostructures of Waugh *et al.*, Crouch *et al.*, and Livermore *et al.*,[2–4] where d is fairly small, about 50 nm (approximately one Fermi wavelength), further circumstantial evidence for $\xi\simeq d$ comes from the fact that the space between the gates that form the interdot barrier is about 100 nm (see Ref. 5). Hence, for these experimental systems, $\hbar\omega$ is approximately $0.2E_F$. Since U is about $0.03E_F$, $2\pi U/\hbar\omega\simeq 1$, within a factor of 2. For experimental systems in which the Fermi wavelength is still about 50 nm but the gates are further from the 2DEG,[19] the ratio $2\pi U/\hbar\omega$ is even larger. On the other hand, both W/E_F and U/E_F are much less than 1, and we can linearize the single-particle energy spectrum about the Fermi surface,

taking $E(j)=E_F+\hbar v_F[k_j-k_F]$, where $k_j=[2mE(j)/\hbar^2]^{1/2}$.

Using the solutions for the wave functions in the vicinity of the parabolic potential,[15,16] we find that $B(j_2,\alpha;j_1,\alpha)\simeq(-1)^{\alpha+1}\sin[\kappa(y_2-y_1)]/2(k_2-k_1)L_{\rm dot}$, and $B(j_2,\overline{\alpha};j_1,\alpha)\simeq(-1)^{\alpha+1}\sin[R(y_2)+R(y_1)]/2(k_2-k_1)L_{\rm dot}$, where $R(y)=(1/2)\arctan(e^{\pi y})$ and $\kappa\simeq 0.1$ for $g\sim 0.1$ with $\kappa\to 0$ as $g\to 0$.

It can be shown that the leading contribution to $\Delta(\rho)$ from same-dot hopping is essentially negligible.[12] The leading contribution from interdot hopping obeys

$$\Delta_T^{(2)}(\rho)\cong-\frac{N_{\rm ch}U}{4\pi^2}\int_0^{\overline{\chi_1}}dx_1\int_0^{\overline{\chi_2}}dx_2\frac{\widetilde{T}(x_1,x_2)}{x_2+x_1+1-\rho}+[\rho\to-\rho],\tag{4}$$

where $\widetilde{T}(x_1,x_2)=\sin^2[\widetilde{R}(Ux_2/\hbar\omega)+\widetilde{R}(-Ux_1/\hbar\omega)]$, $\widetilde{R}(y)=R[y(E_F)+y]$, $\overline{\chi_r}=\hbar v_F\Lambda_r/U$, the symbol $\cong$ signifies equality modulo ρ-independent terms, and the bracketed expression $\rho\to-\rho$ stands for the quantity obtained by replacing ρ by $-\rho$ in the previous term. Ultraviolet cutoffs $\overline{\chi_r}=\hbar v_F\Lambda_r/U$ have been inserted in recognition of the fact that our formulas for the integrands break down at some distance $\Lambda_r\sim 1/\xi$ from the Fermi surface. Since we want the integrals to encompass the range of energies in which $\widetilde{R}(E)$ is rapidly growing, we need $\Lambda_r\gtrsim k_0$, where $E(k_F+k_0)=V_0$ and, consequently, $k_0\xi\simeq(1/2\pi\sqrt{2})\ln[(1-g)/g]$. The requirement $k_0\xi\lesssim 1$ tells us that our calculation gives quantitatively reliable results only for $g\gtrsim 10^{-4}$.

To obtain a result with negligible dependence on the cutoffs $\overline{\chi_r}$, we must have $\overline{\chi_r}\gg 1$. On the other hand, to ensure that the answer is quantitatively reliable, we need $\overline{\chi_r}\lesssim\hbar v_F/U\xi$. Thus, we can only expect quantitatively reliable results for $U\ll\hbar v_F/\xi$; i.e., for $2\pi U/\hbar\omega\ll 2\pi\sqrt{2}$.

From $\widetilde{T}(0,0)=g$, it follows that the limit $2\pi U/\hbar\omega\to 0$ yields the zero-width linear-in-g result that has been derived before.[5,6,8,9] In the limit $2\pi U/\hbar\omega\to\infty$, on the other hand, the shift of Eq. (4) is g independent for g a finite distance from both 0 and 1. Of course, such a result for the limit $2\pi U/\hbar\omega\to\infty$ is only qualitative.

What happens when ξ is between 0 and ∞? By performing two-partial integrations and dropping terms that go to zero as the cutoffs $\overline{\chi_r}$ become infinite, we find that

$$\begin{aligned}\widetilde{f}^{(1)}(\rho)=&\frac{N_{\rm ch}g}{\pi^2}(1-\rho)\ln(1-\rho)\\&+\frac{N_{\rm ch}}{\pi^2}\int_0^{\overline{\chi_1}}dx_1\left[\frac{\partial\widetilde{T}(x_1,0)}{\partial x_1}h(\rho,x_1,0)\right]\\&+\frac{N_{\rm ch}}{\pi^2}\int_0^{\overline{\chi_2}}dx_2\left[\frac{\partial\widetilde{T}(0,x_2)}{\partial x_2}h(\rho,0,x_2)\right]\\&+\frac{N_{\rm ch}}{\pi^2}\int_0^{\overline{\chi_1}}dx_1\int_0^{\overline{\chi_2}}dx_2\frac{\partial^2\widetilde{T}(x_1,x_2)}{\partial x_1\partial x_2}h(\rho,x_1,x_2)\\&+[\rho\to-\rho],\end{aligned}\tag{5}$$

where $h(\rho,x_1,x_2)=(x_2+x_1+1-\rho)\ln(x_2+x_1+1-\rho)$. The first term on the right-hand side of Eq. (5) is the zero-width result. The other terms go to zero when $\xi\to 0$.

Numerical evaluations of Eq. (5) are plotted in Fig. 2(a) for several values of the parameter $2\pi U/\hbar\omega$. A curious feature is that the corrections to the zero-width behavior are antisymmetric about $g=0.5$, a property that can be demonstrated analytically by considering what happens under the transformations $g\leftrightarrow(1-g)$ and $x_1\leftrightarrow x_2$. Though the antisymmetry is suggestive, it must be remembered that $\widetilde{f}^{(1)}(\rho)$ is only the leading term in a perturbative expansion about $g=0$. The small positive contribution to $\widetilde{f}(\rho)$ that comes from the same-dot-hopping shift $\Delta_C^{(2)}$ breaks this antisymmetry, and other higher-order corrections are likely to do the same. Nevertheless, a rough antisymmetry about $g=0.5$ is probably preserved, for, just as $\widetilde{f}(\rho)$ is enhanced at small g by hopping connections to states with large transmission amplitudes, so we expect that $\widetilde{f}(\rho)$ is diminished at large g by the fact that many of the occupied states from which one hops have transmission probabilities smaller than g.

An equivalent expression for Eq. (5) is

$$\widetilde{f}^{(1)}(\rho)=\frac{2N_{\rm ch}\rho^2}{\pi^2}\int_0^{\overline{\chi_1}}dx_1\int_0^{\overline{\chi_2}}dx_2\frac{\widetilde{T}(x_1,x_2)}{(x_2+x_1+1)(x_2+x_1+1-\rho)(x_2+x_1+1+\rho)}.\tag{6}$$

For $g\ll 1$, the magnitude of the $\widetilde{f}^{(1)}(\rho)$ is largely determined by the portion of the integral that corresponds to $x_2\gtrsim x_0$, where $x_0=\hbar v_F k_0/U$. For x_2 in this range, $\widetilde{T}(x_1,x_2)$ is on the order of 1 and therefore much larger than $\widetilde{T}(0,0)$. We label this *high-energy portion* of the double integral $\widetilde{f}^{(1)}_{\rm hep}(\rho)$, where $f^{(1)}_{\rm hep}\sim(N_{\rm ch}/4\pi^2)(2\pi U/\hbar\omega)[1/(|\ln g|+2\pi U/\hbar\omega)]$ for $x_0\gtrsim 1$ and $k_0\lesssim 1/\xi$ or, equivalently, for $(2\pi U)/\hbar\omega\lesssim|\ln g|\lesssim 2\pi\sqrt{2}$.

It is instructive to compare $f^{(1)}_{\rm hep}$ with the zero-width peak splitting, $f^{(1)}_{\xi=0}$. For $2\pi U/\hbar\omega=1$, the ratio $f^{(1)}_{\rm hep}/f^{(1)}_{\xi=0}$ is

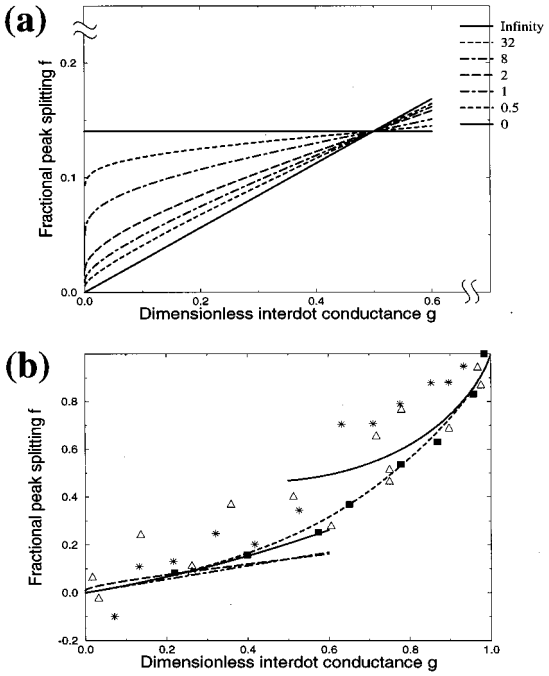

FIG. 2. (a) Plots of the leading $g \to 0$ term of the fractional peak splitting f as a function of the dimensionless interdot channel conductance g for different values of $2\pi U/\hbar\omega$ (see legend on right). All curves are for two interdot tunneling channels, $N_{\rm ch}=2$. The upward sloping solid line is the linear-in-g result for an interdot barrier of effectively zero width ($2\pi U/\hbar\omega=0$). The dashed and dot-dashed curves are for finite-width barriers with $2\pi U/\hbar\omega$ taking values from 0.5 to 32. The horizontal solid line is for an infinite-width barrier. The curves can only be expected to be quantitatively accurate when $2\pi U/\hbar\omega \ll 10$. (b) f-versus-g results for the full domain of g when $N_{\rm ch}=2$. The solid lines are the complete zero-width results in the weak- and strong-coupling limits. These results contain both leading and subleading terms (Ref. 6). The plot for the leading zero-width term in the small-g limit is included as a dot-dashed curve. The small-dashed curve from $(g,f)=(0,0)$ to $(g,f)=(1,1)$ is an interpolating curve derived from the zero-width results. The long-dashed line is the $2\pi U/\hbar\omega=1$ curve of Fig. 2(a). The stars, triangles, and squares represent different sets of experimental data (Refs. 2 and 4), the squares being the most recent (Ref. 4).

roughly 0.6 when $g=0.1$ and 25 when $g=0.001$. Thus, for very weak coupling, the correction to $f^{(1)}_{\xi=0}$ is proportionately very large. At intermediate values of g, the results for $\xi=0$ and $\xi\neq 0$ converge.

Comparison of our results for $f^{(1)}_{\rm hep}$ with the numerical results for $f^{(1)}$ in Fig. 2(a) confirms that $f^{(1)}_{\rm hep}$ captures the essential f-versus-g behavior, particularly as $2\pi U/\hbar\omega$ becomes larger and the exponential enhancement of the tunneling amplitudes becomes more important. The sharp increase in slope as $g \to 0$ can be understood as resulting from the fact that the high-energy portion of the peak splitting is proportional to $(2\pi U/\hbar\omega)/|\ln g|$.

Turning to Fig. 2(b), we examine the significance of the calculated finite-width corrections in the context of the entire f-versus-g curve. The long-dashed curve in Fig. 2(b) is the curve from Fig. 2(a) for the value $2\pi U/\hbar\omega=1$ that appears to characterize the experiments that have supplied the stars, triangles, and squares.[2–4] The dot-dashed line is the leading-order-in-g, zero-width curve from Fig. 2(a). The small-dashed curve is an interpolation for the entire zero-width curve. This interpolation matches both the second-order-in-g calculation of the fractional peak splitting for weak coupling and the two-term calculation for strong coupling, which were obtained in Ref. 6 and are shown as solid curves.

For $2\pi U/\hbar\omega=1$, we see that, although the finite-width correction to f changes the answer by a large factor for small g, the correction is small on an absolute scale. The difference between the dashed curve and the dot-dashed curve never exceeds 0.02 and therefore causes only a small correction to the overall shape of the f-versus-g curve. Qualitatively, the correction due to $\xi\neq 0$ is quite similar to adding a small constant to f near $g=0$ and decreasing the slope of the f-versus-g curve for more intermediate g. This qualitative similarity follows from the fact that the region where f drops rapidly to zero is almost invisible in the plot. Consequently, the correction to the zero-width curve might be hard to distinguish from the effects of a small interdot capacitance, which have already been included in analyzing the data. Introduction of the finite thickness correction therefore has little effect on the agreement between theory and the data in Fig. 2(b), for which $2\pi U/\hbar\omega \simeq 1$. Nevertheless, such corrections may be important in future experiments.

IV. CONCLUSION

By developing an approach to the coupled-dot problem that relies upon the non-interacting, single-particle eigenstates of the full coupled-dot system, we solve for the leading correction to zero-width, weak-coupling results that were derived in previous work.[5,6,8,9] The nonzero barrier width ξ and finite barrier height V_0 mean that the off-diagonal ''hopping terms'' vary exponentially with the energies of the states they connect. For a small interdot channel conductance ($g \ll 1$), the resulting enhancement of tunneling to ''high-energy'' states above the barrier leads to an increase in the magnitude of the fractional peak splitting f observed at a given value of g. For a parabolic barrier, the magnitude of this increase grows with the ratio $2\pi U/\hbar\omega$, where U is the interdot charging energy and ω is the frequency of the inverted parabolic well. Except in a very small region near $g=0$ where f behaves like $(2\pi U/\hbar\omega)/|\ln g|$, the increase in f is accompanied by a decrease in the slope of the f-versus-g curve. The effect upon the overall shape of the f-versus-g curve is not very substantial for $2\pi U/\hbar\omega \simeq 1$ but could be crucial in interpreting experiments involving wider barriers.

One might worry that the finite-width corrections to higher-order terms in the weak-coupling expansion could lead to a more dramatic alteration of the f-versus-g curve. However, the corrections to such ''large-g'' terms should be muted by the fact that, as g increases, there is less difference between tunneling amplitudes between states at the Fermi energy and those between a state at the Fermi energy and a state lying above the barrier.

A more vital source of concern might be the treatment of the electron-electron interactions in the vicinity of the barrier. Clearly, the use of a sharp step function in the equation

for $\hat{n}$ is an artifice. A more realistic model would account for the fact that, though electrons in and about the interdot channel still repel one another locally, their interactions with the rest of the electrons in the system are screened by the surface gates.

Finally, one might wonder whether higher-order corrections to f preserve a rough antisymmetry about $g \simeq 0.5$. Recall that the leading small-g correction, when extended to $g=1$, changes sign and becomes negative for $g>0.5$. Although a proper calculation of the behavior at large values of g requires consideration of higher-order terms, the negativity of the correction to f at large values of g is probably a generally right physical feature. When g is large and the reflection probability at the Fermi energy is small, the energy dependence of the reflection amplitude, for $\xi \neq 0$, should lead to a decrease in f as a result of the enhanced reflection for occupied states lying below the barrier.

The authors thank C. Livermore, C. H. Crouch, R. M. Westervelt, and I. E. Smolyarenko for helpful discussions. This work was supported by the NSF through the Harvard Materials Research Science and Engineering Center, Grant No. DMR94-00396.

[1] For an introduction to the Coulomb blockade, see M. A. Kastner, Rev. Mod. Phys. **64**, 849 (1992); D. V. Averin and K. K. Likharev, in *Mesoscopic Phenomena in Solids*, edited by B. L. Altshuler, P. A. Lee, and R. A. Webb (North Holland, Amsterdam, 1991); various articles in *Single Charge Tunneling*, Vol. 294 of *NATO Advanced Study Institute, Series B: Physics*, edited by H. Grabert and M. H. Devoret (Plenum, New York, 1992); or U. Meirav and E. B. Foxman, Semicond. Sci. Technol. **11**, 255 (1996).

[2] F. R. Waugh, M. J. Berry, D. J. Mar, R. M. Westervelt, K. L. Campman, and A. C. Gossard, Phys. Rev. Lett. **75**, 705 (1995); F. R. Waugh, M. J. Berry, C. H. Crouch, C. Livermore, D. J. Mar, R. M. Westervelt, K. L. Campman, and A. C. Gossard, Phys. Rev. B **53**, 1413 (1996); F. R. Waugh, Ph.D. thesis, Harvard University, 1994.

[3] C. H. Crouch, C. Livermore, F. R. Waugh, R. M. Westervelt, K. L. Campman, and A. C. Gossard, Surf. Sci. **361-362**, 631 (1996).

[4] C. Livermore, C. H. Crouch, R. M. Westervelt, K. L. Campman, and A. C. Gossard, Science **274**, 1332 (1996).

[5] J. M. Golden and B. I. Halperin, Phys. Rev. B **53**, 3894 (1996).

[6] J. M. Golden and B. I. Halperin, Phys. Rev. B **54**, 16 (1996).

[7] The *dimensionless conductance* g is the ''dimensionful'' channel conductance divided by the conductance quantum e^2/h. *Tunneling channel* refers to any distinct orbital or spin tunneling mode.

[8] K. A. Matveev, L. I. Glazman, and H. U. Baranger, Phys. Rev. B **53**, 1034 (1996).

[9] K. A. Matveev, L. I. Glazman, and H. U. Baranger, Phys. Rev. B **54**, 5637 (1996).

[10] C. B. Duke, in *Solid State Physics: Advances in Research and Applications*, edited by H. Ehrenreich and D. Turnbull (Academic, New York, 1969), Suppl. 10.

[11] K. A. Matveev, Phys. Rev. B **51**, 1743 (1995).

[12] J. M. Golden and B. I. Halperin, cond-mat/9611173.

[13] K. A. Matveev and L. I. Glazman, Phys. Rev. B **54**, 10 (1996).

[14] E. Guth and C. J. Mullin, Phys. Rev. **59**, 575 (1941); C. Herring and M. H. Nichols, Rev. Mod. Phys. **21**, 185 (1949); D. W. Juenker, G. S. Colladay, and E. A. Coomes, Phys. Rev. **90**, 772 (1953); K. W. Ford, D. L. Hill, M. Wakano, and J. A. Wheeler, Ann. Phys. (N.Y.) **7**, 239 (1959).

[15] J. N. L. Connor, Mol. Phys. **15**, 37 (1968).

[16] J. C. P. Miller, in *Handbook of Mathematical Functions*, edited by M. Abramowitz and I. A. Stegun, Natl. Bur. Stand. (U.S.) Appl. Math. Ser. No. 55 (U.S. GPO, Washington, DC, 1964), p. 685.

[17] E. C. Kemble, Phys. Rev. **48**, 549 (1935); L. D. Landau and E. M. Lifshitz, *Quantum Mechanics* (Ref. 9), p. 184.

[18] J. H. Davies and J. A. Nixon, Phys. Rev. B **39**, 3423 (1989).

[19] N. C. van der Vaart, A. T. Johnson, L. P. Kouwenhoven, D. J. Maas, W. de Jong, M. P. de Ruyter van Steveninck, A. van der Enden, and C. J. P. M. Harmans, Physica B **189**, 99 (1993); N. C. van der Vaart, S. F. Godijn, Y. V. Nazarov, C. J. P. M. Harmans, J. E. Mooij, L. W. Molenkamp, and C. T. Foxon, Phys. Rev. Lett. **74**, 4702 (1995).